Separation of Metallic and Semiconducting Single-Walled Carbon Nanotube Arrays by "Scotch Tape"**

Guo Hong, Matthew Zhou, Ruoxing Zhang, Shimin Hou, Wonmook Choi, Yun Sung Woo, Jae-Young Choi, Zhongfan Liu, and Jin Zhang*

Single-walled carbon nanotubes (SWNTs) have been regarded as one of the best candidates for future applications in nanoelectronic devices because of their superb electrical characteristics. However, almost all of the currently available technologies can only produce a mixture of both metallic (m) and semiconducting (s) SWNTs. This coexistence in as-grown samples dramatically decreases the device performance; therefore, SWNTs should be separated before they are integrated into devices. During the past decade, two different approaches have been developed to separate m- and s-SWNTs. The first approach is selective destruction by, for example, nitronium ion attack,[1] gas-phase etching reactions,[2] weak oxidative carbon sources,[3] and ultraviolet irradiation.[4] The second strategy involves solution-based methods like dielectrophoresis,[5] density-gradient-inducing centrifugation,[6] selective adsorption of chemicals,[7] and agarose-gel-based separation.[8] Both techniques can separate SWNTs effectively, but the former introduces damages to SWNTs, while the latter can only work for very short SWNTs and creates difficulties in the alignment of SWNTs.

For the purpose of separation, many efforts have been made to investigate selective interactions between chemicals and SWNTs of different conductivities. Electron donor molecules, such as octadecylamine,[9] have been reported to selectively adsorb to s-SWNTs, while aromatic polymers, such

as 9,9-dioctylfluorenyl-2,7-diyl,[10] prefer metallic ones. However, the essential character of these interactions is still unclear. In the case of amines, some researchers think that the interaction is due to the lone pair of the nitrogen atom,[11] while others believe the hydrogen atom is more important.[12] For aromatic polymers, the role of π–π interactions[13] vs. dipole–dipole interactions[14] is controversial. Nevertheless, these adsorption preferences have already been exploited for SWNT separation.

Considering the problems associated with separation techniques such as selective destruction and solution-based methods, our goal was to develop a simple way, which is analogous to mechanical exfoliation of graphene using scotch tape[15] to realize SWNT separation. Specifically, we aimed to create "scotch tapes" terminated with various functional groups that could be used to selectively remove either s- or m-SWNTs and to leave their counterparts on the substrate. Unlike the separation techniques discussed above, this approach was based on the selective adsorption of chemicals to SWNTs of different electrical properties, which can be applied to long SWNTs systems without introducing damage while the SWNTs formation is perfectly maintained.

In our experiments, soft polydimethylsiloxane (PDMS) thin films were chosen as the supporting material, while 3-aminopropyl-triethoxysilane ($C_9H_{23}NO_3Si$, APTES, defined as A-scotch tape) and triethoxyphenylsilane ($C_{12}H_{20}O_3Si$, PTEOS, defined as P-scotch tape) were used as the bonding material to introduce amine and phenyl functional groups, respectively (Figure S1). The Si−O−Si bonds on the PDMS surface were oxidized to Si−OH groups when treated under air plasma. The Si−OH groups could be further reacted with APTES/PTEOS to form strong interactions between the supporting PDMS layer and the functionalized bonding layer.[16] SWNT samples with mixtures of m- and s-SWNTs could be presynthesized on sapphire substrates. As shown in Figure 1, when the PDMS-based "scotch tapes" were applied to SWNT samples and then peeled off, the A-scotch tape selectively removed s-SWNTs, while the P-scotch tape adhered to metallic ones, leaving their counterparts on the substrate.

Single-polished (11–20) plane sapphire substrates (miscut angle < 0.5°, surface roughness < 5 Å) were purchased from Hefei Kejing Materials Technology Co., China and were used for SWNT growth. After an initial cleaning process, substrates were annealed at 1100°C for 10 h so that the aligned SWNT arrays could be grown along the $[1\bar{1}00]$ direction. Growth experiments were performed in a low-pressure chemical vapor deposition (LPCVD) system with a 66 mm quartz tube at a temperature of 850°C and a pressure of 700 torr. A 3 мм

[*] G. Hong, Prof. Dr. Z. F. Liu, Prof. Dr. J. Zhang
Center for Nanochemistry, Beijing National Laboratory for Molecular Sciences, Key Laboratory for the Physics and Chemistry of Nanodevices, State Key Laboratory for Structural Chemistry of Unstable and Stable Species, College of Chemistry and Molecular Engineering, Peking University
Beijing 100871 (China)
Fax: (+ 86) 10-6275-7157
E-mail: jinzhang@pku.edu.cn

M. Zhou
Department of Chemistry, Williams College
Williamstown, MA 01267 (USA)

R. X. Zhang, Prof. Dr. S. M. Hou
School of Electronics Engineering and Computer Science, Peking University
Beijing 100871 (China)

Dr. W. M. Choi, Dr. Y. S. Woo, Dr. J. Y. Choi
Graphene Research Center, Samsung Advanced Institute of Technology
San 14-1, Nongseo-Dong, Giheung-Gu, Yongin, Gyeonggi-Do 446-712 (Korea)
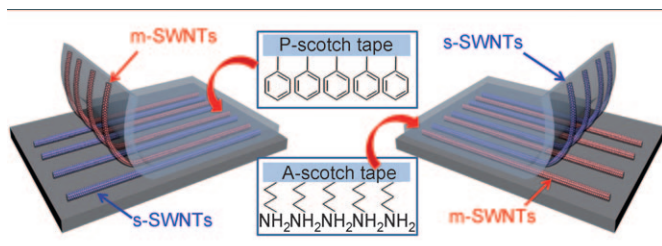
Figure 1. Schematic of SWNT separation using P- and A-scotch tapes to selectively remove m- and s-SWNTs respectively, and leave their counterparts on the sapphire substrates.

Fe(OH)$_3$/ethanol solution was used as the catalyst, and was spin coated onto the substrate surface. The substrate was heated to the desired temperature in air and was kept in a gas flow of 2200 sccm of argon and 500 sccm of hydrogen for catalyst reduction for 5 min, followed by 5 min of 2200 sccm of argon, 500 sccm of hydrogen, and 50 sccm of ethanol purged with argon to grow SWNTs at an average density of 10 tubes/μm, or 4 min of 2200 sccm of argon, 500 sccm of hydrogen and 45 sccm of ethanol purged with argon for an average density of 2 tubes/μm.

The silicone elastomer base and its curing agent were purchased from Dow Corning Corporation, USA and they were mixed in a 10:1 ratio by mass. After stirring for 20 min, the mixture was kept still for 1 h (no agitation) to remove air bubbles. Microscope slides were cleaned by sonication in deionized water/acetone/ethanol/deionized water in turn and were used as templates to generate flat PDMS surfaces. The mixture solidified after baking in an oven at 90 °C for 1 h to give an elastomeric PDMS film. Solidified PDMS films were peeled off of the glass templates immediately before deco-

ration to avoid surface contamination, and were treated under air plasma at a power of 90 W and a gas flow of 15 sccm. The treatment time was set as 5 min, 10 min, or 15 min, depending on the conditions tested. APTES and PTEOS were dispersed in ethanol at concentrations of 1%, 5%, 10%, 20%, and 30% by mass. After plasma treatment, a given PDMS film was immersed in the appropriate solution for 10 min and then rinsed with ethanol to remove unreacted triethoxysilane. After drying in air for about 5 min, the scotch tape was ready for use.

In the case of m-SWNT separation, A-scotch tape was used to selectively remove s-SWNTs. For better comparison of the separation results, only half of each SWNT sample was treated, as shown in Figure 2a, creating three different regions on the sample: as-grown, treated, and boundary. After peeling off the scotch tape, clear density differences between as-grown and treated regions were observed in SEM (Figure 2b). This phenomenon did not occur for bare and plasma-treated PDMS, or bare, plasma-treated, and APTES-decorated SiO$_2$/Si substrates. AFM images of as-grown (Figure 2c) and treated (Figure 2d) regions indicated that the alignment of the SWNT arrays was maintained. Radial breathing mode (RBM) signals of SWNTs in Raman spectra (632.8 nm excitation) were used to characterize the distribution of m- and s-SWNTs in each region. In the as-grown regions (Figure 2e), plenty of m- and s-SWNT signals were collected, while in the treated regions (Figure 2f), , proportionally more m-SWNT signals were observed, according to the Kataura plot.[17] These results suggested that the A-scotch tape can selectively remove s-SWNTs, and leave their counterparts on the sample substrate.

For the separation of s-SWNTs, P-scotch tape was used to selectively remove m-SWNTs. As shown in Figure 3a, only half of each SWNT sample was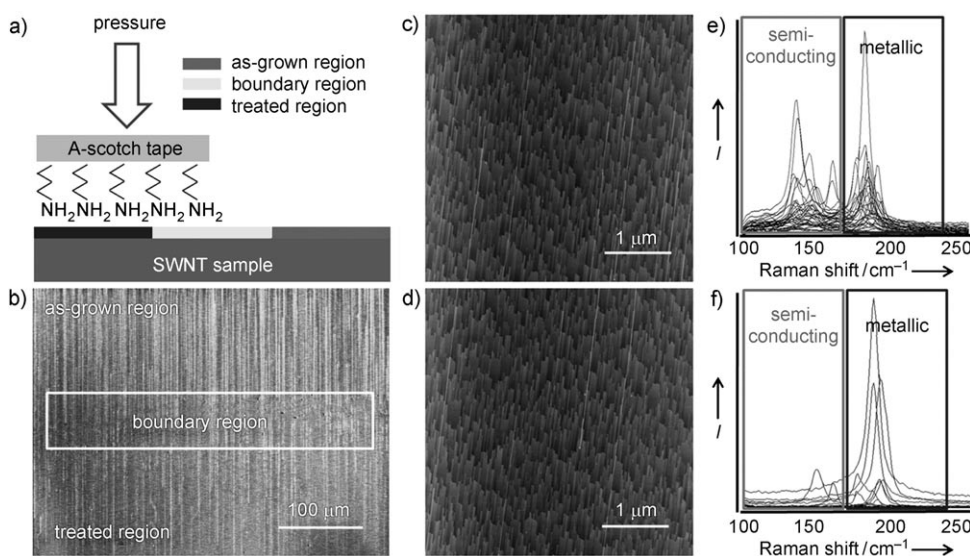 treated, again to facilitate the interpretation of the separation results. After peeling off the scotch tape, clear density differences between as-grown and treated regions were also observed in SEM (Figure 3b). In control experiments, neither bare and plasma-treated PDMS, nor bare, plasma-treated, and PTEOS-decorated SiO$_2$/Si substrates could remove any SWNTs at all. AFM images from as-grown (Figure 3c) and treated (Figure 3d) regions also indicated perfect maintenance of SWNT alignment. In the as-grown regions (Figure 3e), plenty of m- and s-SWNT signals were collected, while in the treated regions (Figure 3f), proportionally more s-SWNT signals were observed in Raman spectra. These results showed that P-
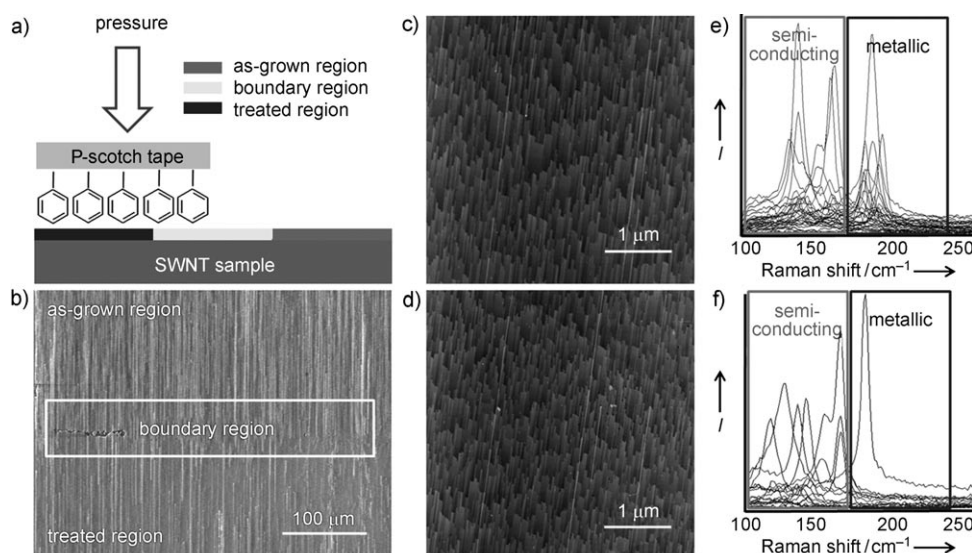

Figure 2. Separation process and corresponding characterization results for the A-scotch tape. a) Schematic of separation process for A-scotch tape. Only half of each SWNT sample was treated, creating three different regions on the substrate. b) SEM image of the boundary region after treatment. c,d) AFM images collected at as-grown (c) and treated (d) regions. e,f) Raman spectra collected at as-grown (e) and treated (f) regions.

Figure 3. Separation process and corresponding characterization results for P-scotch tape. a) Schematic of separation process for P-scotch tape. Only half of each SWNT sample was treated, creating three different regions on the substrate. b) SEM image of boundary region after treatment. c,d) AFM images collected at as-grown (c) and treated (d) regions. e,f) Raman spectra collected at as-grown (e) and treated (f) regions.

scotch tapes can selectively remove m-SWNTs and leave their counterparts on the sample substrate.

To optimize the separation results, a series of experiments investigating plasma time and bonding material concentration were run with the goal of changing the effective number of functional groups associated with the bonding materials. Seven conditions were chosen with plasma time [min]/ bonding material concentration [%] varied as 0/0 (0), 1/1 (1), 5/10 (2), 10/10 (3), 10/20 (4), 15/20 (5), and 15/30 (6). For each condition, a number ranging from 0 to 6 is assigned in Figure 4a–d. After peeling off the scotch tape of the sample substrate, SWNT densities in as-grown and treated regions were collected by SEM for each condition. The density changes were reported in Figure 4a (A-scotch tape) and Figure 4b (P-scotch tape). It was found that under the 10/20 condition, A-scotch tape could remove most SWNTs, while the 10/10 condition was most effective for P-scotch tape. Corresponding m-/s-SWNT distributions were characterized by Raman spectroscopy and are given in Figure 4c (A-scotch tape) and Figure 4d (P-scotch tape). Circles represent as-grown regions while triangles represent treated regions. The results of both SEM and Raman spectroscopy show that the best A-scotch tape was fabricated using the 10/20 condition, while the 10/10 condition was the best one for the P-scotch tape.

To further confirm this result, SWNT samples treated under the best conditions were transferred onto SiO_2/Si substrates by applying the peel-off method[18] and were incorporated into field effect transistors (FET). Electron beam lithography (EBL) was used to identify electrode structure and location. Figure 5a gives the optical and SEM images of the electrode structure. Electrical measurements were performed with a 100 mV bias voltage and 5 μm channel width. In cases where multiple tubes existed in one FET structure, current break was performed to help identify the

SWNT electrical properties.[19] As shown in Figure 5b, the SWNT arrays obtained after treatment by A-scotch tape consisted of about 90% m-SWNTs while in Figure 5c, the SWNT arrays obtained after treatment by P-scotch tape contained 85% s-SWNTs.

First-principles calculations were performed to gain insight into the selectivity of amine- and phenyl-terminated surfaces, which were modeled by $NH_2-(CH_2)_3-SiH_3$ and $C_6H_5-SiH_3$ molecules, respectively. (8, 8) and (14, 0) SWNTs were chosen as representative m- and s-SWNTs. The calculations were based on DFT with the Perdew–Zunger local density approximation (LDA) as the exchange-correlation functional.[20] As shown in Figure 6a for (8, 8) and Figure 6b for (14, 0) SWNTs, the same most-stable geometry for the $NH_2-(CH_2)_3-SiH_3$ molecule was obtained when the N atom was in the center of the six-member ring and its lone pair was perpendicular to the SWNT surface, with respective binding energies of 203 and 214 meV. However, the
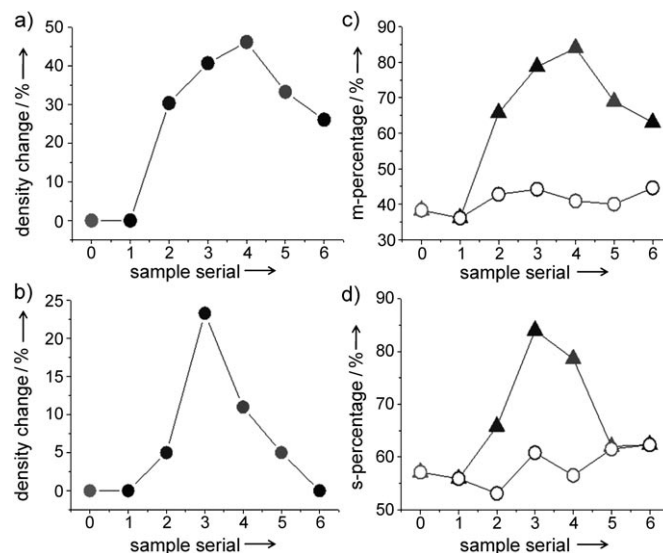

Figure 4. Optimization of separation results for A- and P-scotch tape. a,b) Density changes after application of each condition for A- (a) and P- (b) scotch tape. c,d) SWNT percentages characterized by Raman spectroscopy at as-grown (circles) and treated (triangles) regions for A- (c) and P- (d) scotch tapes. Seven conditions, with variation of the plasma time [min]/bonding material concentration [%] given as 0/0 (0), 1/1 (1), 5/10 (2), 10/10 (3), 10/20 (4), 15/20 (5), and 15/30 (6). For each condition, a number ranging from 0 to 6 is assigned. The average density of as-grown samples was 10 tubes/μm for the A-scotch tape and 2 tubes/μm for the P-scotch tape.
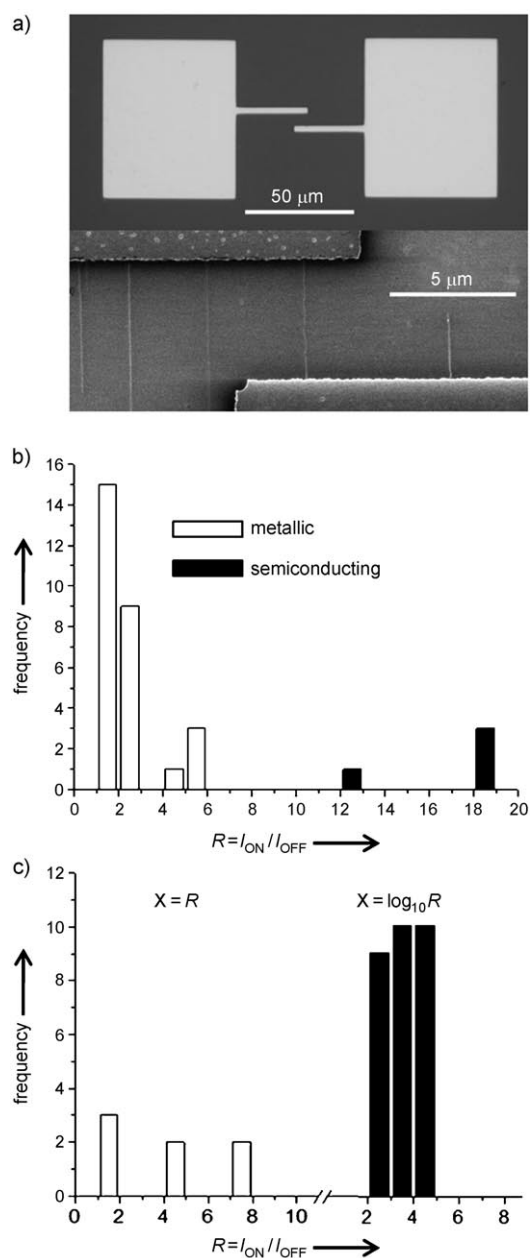
Figure 5. Electrical measurements of separated samples. a) Optical and SEM images of the electrode structure. b) Electrical measurements of SWNT samples after treatment with A-scotch tapes. c) Electrical measurements of SWNT samples after treatment with P-scotch tapes. The white bars represent m-SWNTs, while the black bars represent s-SWNTs. In cases in which multiple tubes existed in one FET structure, current break was performed to help identify the SWNT electrical properties.

Figure 6. The lowest-energy configurations of silanes adsorbed on SWNTs. a) The $NH_2-(CH_2)_3-SiH_3$ molecule near the hollow center of the (8, 8) SWNT. b) The $NH_2-(CH_2)_3-SiH_3$ molecule near the hollow center of the (14, 0) SWNT. c) The stacked configuration of the $C_6H_5-SiH_3$ molecule on the (8, 8) SWNT. d) The bridge configuration of the $C_6H_5-SiH_3$ molecule on the (14, 0) SWNT.

most stable adsorption geometries for the phenylsilane molecule were a stacked configuration on (8, 8) SWNTs and a bridge configuration for (14, 0) SWNTs (Figure 6c and d),[21,22] with corresponding binding energies of 432 and 416 meV. This calculation indicated that amine-terminated surfaces have stronger interactions with s-SWNTs, while phenyl-terminated surfaces prefer metallic ones, which is qualitatively consistent with our experimental findings. Considering the one-di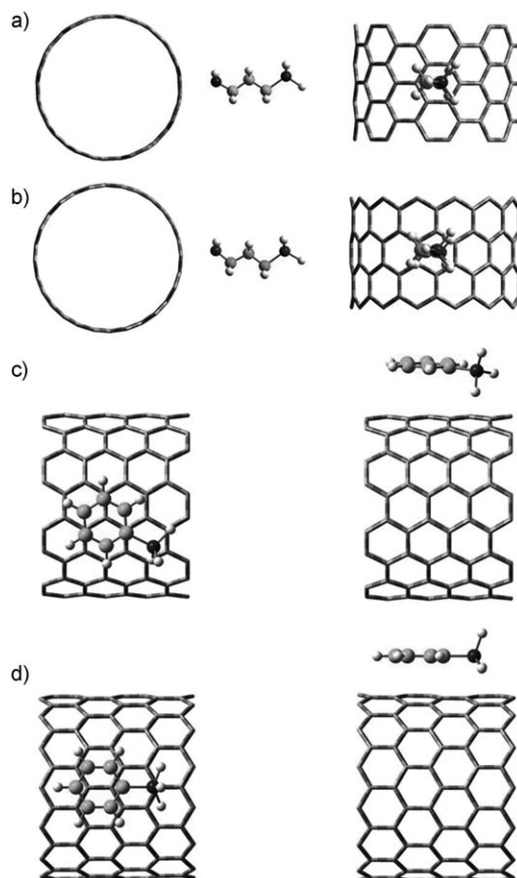mensional character of SWNTs, the adsorption difference will enhance with SWNT length, because the average length of the SWNTs was several hundreds of micrometers. Given that the density change for P-scotch tape was significantly smaller than that for A-scotch tape, the phenyl group was probably neither perpendicular nor parallel to the SWNT side wall, but interacted at an angle alterable by experimental parameters and thus the dipole–dipole interactions might be more reasonable.

For any kind of scotch tape discussed above, the strength of the interaction with SWNTs should be proportional to the density of the effective bonding material functional groups on it. As amine functional groups are hydrophilic while phenyl functional groups are hydrophobic, contact-angle characterizations were used to explain the scotch tape quality (Figure S2). In the scotch tape fabrication process, hydrophobic Si−O−Si moieties on a PDMS surface were transformed into hydrophilic Si−OH groups under air plasma, so the observed contact angles first decreased with increased exposure to plasma. After a treatment of 5 min, further oxidation lead to an increase of the contact angle, likely due to surface damage. At a given time of the plasma treatment (such as 10 or 15 min), higher concentrations of APTES solution led to smaller contact angles, while higher PTEOS concentrations led to

larger ones. This result indicated higher effective functional group density on the surface. Moreover, since the interactions are at their maximum when phenyl functional groups are parallel rather than perpendicular to the SWNTs, it is reasonable that the best condition for the P-scotch tape was 10/10, rather than 10/20 as seen for A-scotch tape. However, the dramatic contact angle increase after 15 min of treatment with plasma suggested that the PDMS surface was damaged to the point that the performance was poor even with higher triethoxysilane concentrations.

In addition to the two parameters discussed above, density and sidewall conditions of SWNTs should also be taken into consideration. The fabrication conditions determine the amount of effective bonding material functional groups on the scotch tape surface, which then determine the number of SWNTs that could be removed and thus the separation result. In general, the higher the SWNT density, the poorer the separation will be, when keeping all other conditions unchanged. Moreover, since the separation mechanism is based on the interaction between amine/phenyl functional groups and SWNTs, any contamination, such as amorphous carbon introduced during SWNT synthesis, should weaken the separation effect. The separation protocol was repeated several times on one sample with a density of 40 tubes/μm using the A-scotch tape (Figure S3). In the first round, the percentage of m-SWNTs increased by 11.7% (from 43.5% to 55.2%), while in the second round, it increased by an additional 5.3% (from 55.2% to 60.5%). However, the percentage of m-SWNTs decreased by 9.7% (from 60.5% to 50.8%) in the third round, which might have been due to contamination introduced in the first and second rounds. Since amine groups prefer s-SWNTs, residual APTES molecules left on the sample substrate from previous trials could protect s-SWNTs and lead to removal of more m-SWNTs.

In conclusion, we developed a simple method to separate m- from s-SWNTs by using chemically modified PDMS thin films as "scotch tape". Unlike with the selective destruction methods, there was no damage introduced to the SWNTs during the separation process. Moreover, SWNT alignment can be perfectly maintained and there is no limitation to SWNT length, since the technique is not solution based. This method is also useful for SWNT separation over large areas, as the PDMS films are simple to synthesize.

[1] K. H. An, J. S. Park, C. M. Yang, S. Y. Jeong, S. C. Lim, C. Kang, J. H. Son, M. S. Jeong, Y. H. Lee, *J. Am. Chem. Soc.* **2005**, *127*, 5196–5203.

[2] G. Y. Zhang, P. F. Qi, X. R. Wang, Y. R. Lu, X. L. Li, R. Tu, S. Bangsaruntip, D. Mann, L. Zhang, H. J. Dai, *Science* **2006**, *314*, 974–977.

[3] L. Ding, A. Tselev, J. Y. Wang, D. N. Yuan, H. B. Chu, T. P. McNicholas, Y. Li, J. Liu, *Nano Lett.* **2009**, *9*, 800–805.

[4] G. Hong, B. Zhang, B. H. Peng, J. Zhang, W. M. Choi, J. Y. Choi, J. M. Kim, Z. F. Liu, *J. Am. Chem. Soc.* **2009**, *131*, 14642–14643.

[5] R. Krupke, F. Hennrich, H. von Lohneysen, M. M. Kappes, *Science* **2003**, *301*, 344–347.

[6] M. S. Arnold, A. A. Green, J. F. Hulvat, S. I. Stupp, M. C. Hersam, *Nat. Nanotechnol.* **2006**, *1*, 60–65.

[7] M. C. LeMieux, M. Roberts, S. Barman, Y. W. Jin, J. M. Kim, Z. N. Bao, *Science* **2008**, *321*, 101–104.

[8] T. Tanaka, H. Jin, Y. Miyata, S. Fujii, H. Suga, Y. Naitoh, T. Minari, T. Miyadera, K. Tsukagoshi, H. Kataura, *Nano Lett.* **2009**, *9*, 1497–1500.

[9] D. Chattopadhyay, I. Galeska, F. Papadimitrakopoulos, *J. Am. Chem. Soc.* **2003**, *125*, 3370–3375.

[10] A. Nish, J. Y. Hwang, J. Doig, R. J. Nicholas, *Nat. Nanotechnol.* **2007**, *2*, 640–646.

[11] J. Kong, H. J. Dai, *J. Phys. Chem. B* **2001**, *105*, 2890–2893.

[12] J. Lu, L. Lai, G. F. Luo, J. Zhou, R. Qin, D. Wang, L. Wang, W. N. Mei, G. P. Li, Z. X. Gao, S. Nagase, Y. Maeda, T. Akasaka, D. P. Yu, *Small* **2007**, *3*, 1566–1576.

[13] S. Gotovac, H. Honda, Y. Hattori, H. Takahashi, H. Kanoh, K. Kaneko, *Nano Lett.* **2007**, *7*, 583–587.

[14] X. Y. Pan, L. J. Li, M. B. Chan-Park, *Small* **2010**, *6*, 1311–1320.

[15] K. S. Novoselov, A. K. Geim, S. V. Morozov, D. Jiang, Y. Zhang, S. V. Dubonos, I. V. Grigorieva, V. V. Firsov, *Science* **2004**, *306*, 666–669.

[16] J. J. Feng, A. J. Wang, J. Fan, J. J. Xu, H. Y. Chen, *Anal. Chim. Acta* **2010**, *658*, 75–80.

[17] A. Jorio, R. Saito, J. H. Hafner, C. M. Lieber, M. Hunter, T. McClure, D. Dresselhaus, M. S. Dresselhaus, *Phys. Rev. Lett.* **2001**, *86*, 1118–1121.

[18] L. Y. Jiao, X. J. Xian, Z. Y. Wu, J. Zhang, Z. F. Liu, *Nano Lett.* **2009**, *9*, 205–209.

[19] P. G. Collins, M. S. Arnold, P. Avouris, *Science* **2001**, *292*, 706–709.

[20] J. P. Perdew, A. Zunger, *Phys. Rev. B* **1981**, *23*, 5048–5079.

[21] F. Tournus, J. C. Charlier, *Phys. Rev. B* **2005**, *71*, 165421.

[22] F. Tournus, S. Latil, M. I. Heggie, J. C. Charlier, *Phys. Rev. B* **2005**, *72*, 075431.